Atomic-scale tuning of self-assembled ZnO microscopic patterns: from dendritic fractals to compact island

Chen Li,[a] Guo Li,[a] Chengmin Shen,[a] Chao Hui,[a] Jifa Tian,[a] Shixuan Du,[a] Zhenyu Zhang[bcd] and Hong-Jun Gao*[a]

Received 19th June 2010, Accepted 14th July 2010
DOI: 10.1039/c0nr00421a

How nature uses water molecules to create fascinating patterns ranging from snowflakes to ice cubes has intrigued mankind for centuries. Here we use ZnO to mimic nature's versatility in creating microscopic patterns with tunable morphology. During growth of ZnO on Zn-dominant spheres *via* chemical vapor deposition, highly regular and symmetric dendritic snowflake patterns and smooth compact islands can be obtained at different growth conditions. We reproduce the dendritic patterns using atomistic Monte Carlo simulations. These findings not only improve understanding of how water molecules form various patterns, but may also be instrumental in tailoring ZnO nanostructures for desirable functionality.

Perpetual effort is made by mankind in trying to understand and mimic nature's versatility in creating various enchanting patterns. Such efforts often involve prototypical atoms or molecules as building blocks, with water molecules and carbon atoms as prime examples.[1–5] More recently, a rich variety of morphological patterns have been discovered from ZnO-based structures,[6] including nanobelts,[7] nanowires,[8] nanosprings,[9] and nanorings.[10] Here we substantially broaden the morphological phase space reachable with Zn and O as the basic constituent elements. We show that, under the proper growth conditions, highly regular and symmetric dendritic snowflake patterns of varying compactness can be obtained at different ZnO coverages. Furthermore, a reduction in the relative concentration of oxygen supply leads to smooth compact islands with sharp or flat tops. These ZnO-based morphological patterns closely resemble those of a water molecule. We therefore expect that the underlying formation mechanisms revealed *via* Monte Carlo simulations should also be instrumental to the understanding of the fascinating patterns made by water in nature.

The synthesis was carried out in a conventional furnace with a horizontal quartz tube.[11,12] Zinc powder (99.99%) was milled in an agate mortar for 20 min prior to being put into a quartz boat covered with a silicon (111) substrate. When the center of the tube furnace reached 800 °C, the boat containing the zinc powder was placed inside and heated for 5 min. The varied surface morphologies of the microscopic-scale spheres were prepared by controlling the composition of the atmosphere and the cooling rate upon their removal from the furnace.

A field-emission scanning electron microscope (FE-SEM) (XL-SFEG, FEI Corp) was used to observe the morphologies of ZnO on Zn-dominant spheres. X-ray diffraction (XRD) data was obtained on a Rigaku D/MAX 2400 type spectroscope with Cu $K_{\alpha 1}$ radiation (wavelength 1.5406 Å). The photoluminescence (PL) measurement was performed at room temperature on a Renishaw Raman spectrometer with He–Cd laser excitation light of an excitation wavelength of 325 nm.

Representative SEM images are shown in Fig. 1. The patterns shown in Fig. 1(a), (b) and (c) were obtained by cooling down the

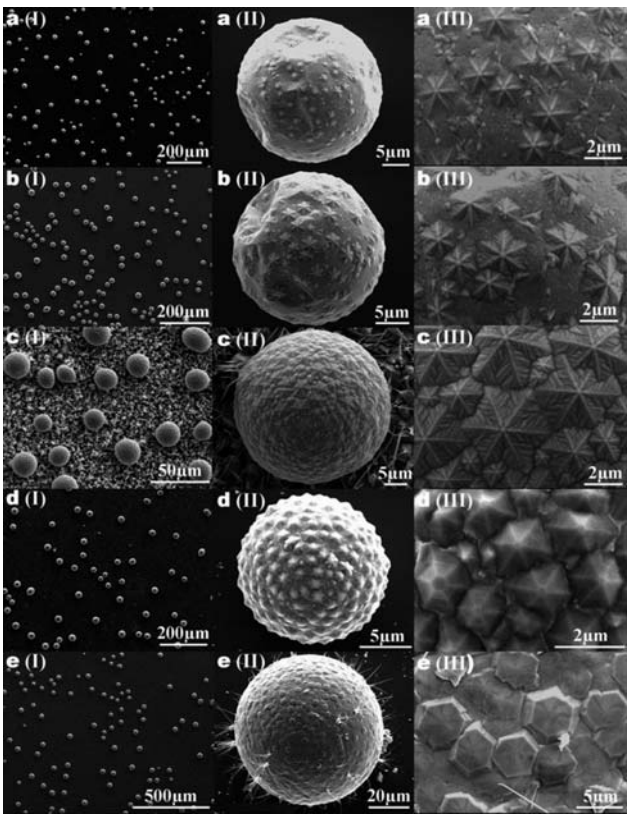

Fig. 1 SEM images of varied morphology of microscopic-scale spheres synthesized under different conditions. The five SEM images (a(I)-e(I)) of low magnification in the left column show the large scale of spheres. The five SEM images in the middle column (a(II)-e(II)) show their corresponding single 3D superstructure. The five SEM images in the right column (a(III)-e(III)) show the diverse morphology of ZnO snowflake patterns on the microsphere. The surface of the microsphere: (a), (b) and (c) have snowflake-like hexagonal structures of different densities; (d) has the truncated-pyramid tips structure; and (e) has the hexagonal plates structure.

[a]*Institute of Physics, Chinese Academy of Sciences, Beijing, 100190, P R China. E-mail: hjgao@iphy.ac.cn*
[b]*Oak Ridge National Laboratory, Oak Ridge, USA*
[c]*University of Tennessee, Knoxville, USA*
[d]*ICQD, the University of Science and Technology of China, Hefei, Anhui, P R China*

Zn-dominant spheres to room temperature in air with cooling rates of 800 °C min^{-1}, 300 °C min^{-1} or 150 °C min^{-1}, respectively. The patterns shown in Fig. 1(d) and (e) were synthesized with similar growth conditions, except that the cooling atmosphere was modified with an influx of Ar, resulting in a reduced concentration of oxygen in the chamber; the corresponding cooling rates were about 150 °C min^{-1} and 5 °C min^{-1}, respectively. The five low-magnification SEM images in the left column show the distributions of the three-dimensional (3D) microscopic-scale spheres on the substrate. The five SEM images in the middle column show the corresponding morphology of a single 3D sphere from each case, and the five SEM images in the right column depict the patterns present on the surface of the individual microsphere in greater detail. From the SEM images in the right column, we observe that the surfaces of the microspheres shown in Fig. 1(a) are sparsely covered by highly symmetric hexagonal dendritic structures. Each of the six branches of the dendrite has the same thin Christmas-tree shape, and their lengths are approximately the same. This snowflake-like hexagonal structure increases in both size and density of the branches in Fig. 1(b). In Fig. 1(c), the snowflake-like structures on the surface of the microsphere are shaped such that the surface is uniformly covered. Two other types of patterns are shown in Fig. 1(d) and Fig. 1(e). Fig. 1(d) shows a variety of microspheres which are covered by truncated-pyramid tips, and Fig. 1(e) depicts microspheres covered with hexagonal plates.

The structure and composition of these spheres were analyzed by X-ray diffraction (XRD) and energy dispersive X-ray spectroscopy (EDX). In the XRD pattern, diffraction peaks of both ZnO and Zn have been observed, indicating the microspheres consist of both Zn and ZnO (Fig. 2(a)). The XRD pattern shows that all of the peaks are sharp and have narrow full width at half maximum (FWHM). These reflection peaks match well with patterns of ZnO (JCPDS, No, 80-0075) and Zn (JCPDS, No, 04-0831). In order to get more information about the microspheres, EDX was used to investigate the components of their surface and interior. The results are shown in Fig. 2(b). The EDX result from the snowflake-like hexagonal surface of the microsphere (Fig. 2 b(II)), which shows only elements Zn and O, proves the presence of the ZnO. We used FIB (Focused Ion Beam, FEI DB235) to etch the surface of each type of microsphere to expose its interior (Fig. 2 b(I)). EDX analysis (Fig. 2 b(III)) of the interior reveals that the core is only Zn, with the presence of Si caused by the sputtering of the Si substrate in the etching process. EDX measurements were made of both the hexagonal and the smooth portions of the microsphere partially covered by snowflake-like hexagonal structures (Fig. 2 c(I)). Oxygen exists only in the snowflake-like hexagonal structure (Fig. 2 c(II)) and is not found in the smooth part of the sphere (Fig. 2 c(III)). The results of the other four types of structures were similar, further demonstrating that the microspheres are composed of a pure Zn interior and surface with ZnO only present in the snowflake-like structures.

The room-temperature photoluminescence (PL) spectra of ZnO on Zn-dominant spheres were measured with the excitation from 325 nm emission laser with 1 mW power (the intensity is about 450 W cm^{-2}). Fig. 3 illustrates the PL spectra of ZnO on Zn-dominant spheres of different coverage percentages and morphologies on the surface. The curves a, b, and c in Fig. 3 correspond to Zn-dominant spheres, sparsely covered by ZnO snowflake-like hexagonal patterns (Fig. 1 a(II)), partly covered by snowflake-like hexagonal structure (Fig. 1 b(II)), and entirely covered by planar hexagons (Fig. 1 e(II)),

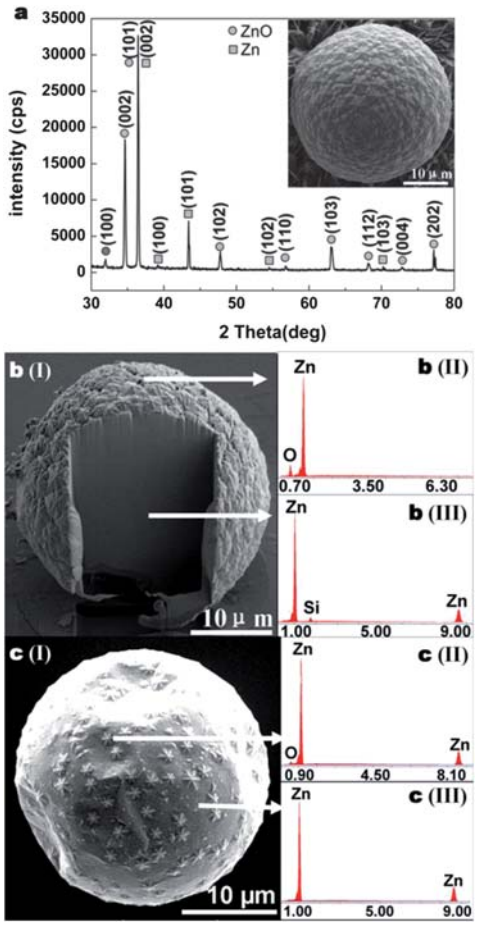

Fig. 2 Structure and composition analyses of microscopic-scale spheres. (a) XRD results of the spheres covered by snowflake-like hexagonal patterns, showing the coexistence of Zn and ZnO. b(I) A ZnO on Zn-dominant microsphere covered by snowflake-like hexagonal patterns etched by FIB. b(II) EDX results of the surface of b(I), showing the existence of O. b(III) EDX results of the core of b(I), showing that there is only Zn. c(I) A microsphere partly covered by snowflake-like hexagonal patterns. c(II) EDX results of the snowflake part of c(I), showing the existence of O. c(III) EDX results of the smooth part of c(I) showing that there is only Zn.

respectively. A UV emission band peak located at about 380 nm and a broad green peak referring to a deep-level or trap-state emission at about 530 nm were detected. The feature at about 380 nm corresponds to the near-band-gap emission, and the broad peak at 530 nm is attributed to single-ionized oxygen vacancies in ZnO. In the 4× magnification PL spectra, it can be observed that the UV emission band at 376 nm of the microspheres partly covered by snowflake structures is blue-shifted compared with those sparsely covered by snowflake structures (378 nm). This result shows that the degree of surface coverage of snowflake-like ZnO on the surface of Zn microspheres can affect the optical properties of the materials. It is found that the intensities of the ultraviolet excitation and the green emission of the spheres covered by snowflake structures are nearly the same, indicating that more oxygen vacancies exist in these structures. Compared to snowflake-like ZnO/Zn microspheres, the microspheres covered by planar hexagons exhibit a stronger luminescence. The PL peak at 383 nm is 12 times that of the snowflake-like ZnO/Zn structures. This peak can be assigned to an excitonic transition indicating that the hexagonal structures can improve the crystal

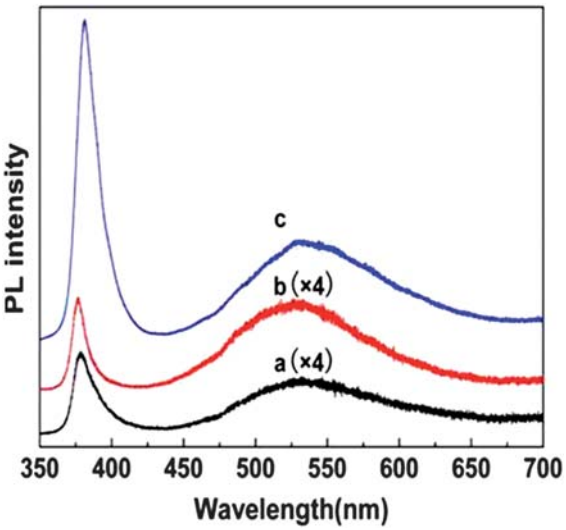

Fig. 3 Room-temperature PL spectra of ZnO on Zn-dominant spheres. (a) Sparsely covered by snowflake-like hexagonal patterns. (b) Partly covered by snowflake-like hexagonal structures. (c) Entirely covered by planar hexagons.

quality of the ZnO, which implies fewer structural defects and a fine crystalline form in the hexagonal structures. These results prove that the fabrication of novel ZnO/Zn structures is an important way to tailor the physical properties of semiconductor materials.[13]

The variety of growth patterns obtained experimentally resembles snowflakes, and the knowledge about the formation of these patterns may provide a better understanding of the mechanisms behind the growth of natural snowflakes.[14] For the dendritic patterns, we investigated the growth processes using Monte Carlo simulations in the nonequilibrium growth region.[15–20] In the simulations, a fixed range with a nucleation center was set, with the range about the size of the ZnO islands in the experiments. Periodical conditions were used and particles were added one by one into the region. A particle on the Zn surface continues to diffuse until reaching the edge of the ZnO island. If the particle is at a kink site (with more than 2 nearest neighbors) or on the ZnO surface, it will stop and become part of the growing aggregate. If the particle is at the straight part of the island edge (namely, with no more than 2 nearest neighbors), it will stop with a probability p, which is connected to the expected total number of hops n *via* the relation

$$\langle n\rangle = \sum_{n=0}^{\infty} np(1-p)^{n-1} = \frac{1}{p} \quad (1)$$

Accordingly, the expected diffusion length is given by

$$\langle |S|\rangle = a\sqrt{\frac{2\langle n\rangle}{\pi}} = a\sqrt{\frac{2}{\pi p}} \quad (2)$$

Here, $a = 3.25$ Å is the lattice constant of ZnO (001). The diffusion length may change during the growth, but this does not affect the main simulation results. Therefore, as a simplification, we set $p = 0.0005$, i. e. $\langle |S|\rangle = 11.6$ nm. Moreover, in the growth, different cooling rates result in different growth time, then different coverages. Here, we use coverage to demonstrate the effect of cooling rates.

The simulation results are shown in the right column of Fig. 4. The corresponding coverages from up to down are 13%, 52% and 100%,

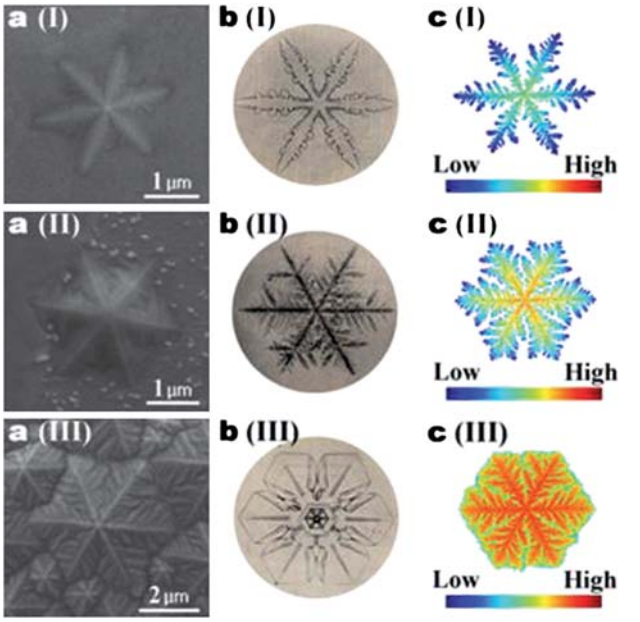

Fig. 4 ZnO patterns, natural snowflakes and simulation results. a(I–III) The different patterns observed in the experiment. b(I–III) Different types of snowflakes in ref. 14, b(I) is photo 6 of p. 18, b(II) is photo 3 of p. 18 and b(III) is photo 6 of p. 21. c(I–III) The simulated results.

respectively. It is found that the dendritic patterns are mainly modulated by the total coverage. When the coverage is low, there is plenty of void space between the islands. Most of the particles attaching to the islands reach the islands from the outside "shores" rather than in the "bays". Because of the screening effect,[21] the main branches grow quickly but the growth of the side branches is highly restrained. When the coverage is larger, there is less void space between the islands, so most of the incoming particles are deposited in the bays between the main branches. Therefore, compared with the main branches, the side branches grow proportionally faster. If the coverage reaches a full monolayer, all the sites are occupied, and have nearly the same growth speed in the direction perpendicular to the surface. In this case, the dendritic snowflake-like patterns remain the same in the lateral directions but increase their heights vertically.

The formation mechanism of the more compact patterns is too complicated to simulate on equal atomistic footing, but a possible mechanism is proposed as follows: The patterns grow with an influx of Ar gas, resulting in a rapid decrease in the concentration of oxygen. The cooling rates for these patterns are lower than those of the growth of the dendritic patterns. Therefore, since the diffusion length is larger, effective corner crossing of a particle diffusing along the island edges is more frequent. This results in patterns that are compact rather than dendritic.[22,23]

Conclusions

In summary, we have mimicked the naturally created snow and ice crystal patterns from dendrites to plates in ZnO/Zn hetero-nanostructures. The underlying mechanism is revealed by detailed atomistic Monte Carlo simulations of the growth processes in the nonequilibrium regime pointing to the crucial role of different coverages of the aggregates. The present work is helpful for revealing the atomic scale processes that give rise to our micrometre-scale

"snowflakes" and shed new light on the formation of natural millimetre-scale snowflakes and ice crystals.

Acknowledgements

We thank Brandon Bell for a critical reading of the ms. The project was supported in part by the National Natural Science Foundation of China, National "863" and "973" programs of China and the Chinese Academy of Sciences, and in part by the Division of Materials Sciences and Engineering, Office of Basic Energy Sciences, U.S. Department of Energy, and by the U.S. National Science Foundation with grant # DMR-0906025.

Notes and references

1 Y. Han, *Han Shi Wai Zhuan*, China, 135 BC.
2 J. Kepler, *The Six-Cornered Snowflake*, Godfrey Tampach, Frankfurt, 1611.
3 R. Descartes, *Meteorlogia*, Amsterdam, 1635.
4 G. Hellmann, *Schneekrystalle*, Verlag Rudolf Mfickenberger, Berlin, 1893.
5 J. Carrasco, A. Michaelides, M. Forster, S. Haq, R. Raval and A. Hodgson, *Nat. Mater.*, 2009, **8**, 427–431.
6 U. Ozgur, Y. I. Alivov, C. Liu, A. Teke, M. A. Reshchikov, S. Dogan, V. Avrutin, S. J. Cho and H. Morkoc, *J. Appl. Phys.*, 2005, **98**, 041301-1-103.
7 Z. W. Pan, Z. R. Dai and Z. L. Wang, *Science*, 2001, **291**, 1947–1949.
8 Y. Li, G. W. Meng, L. D. Zhang and F. Phillipp, *Appl. Phys. Lett.*, 2000, **76**, 2011–2013.
9 X. Y. Kong and Z. L. Wang, *Nano Lett.*, 2003, **3**, 1625–1631.
10 X. Y. Kong, Y. Ding, R. S. Yang and Z. L. Wang, *Science*, 2004, **303**, 1348–1351.
11 J. F. Tian, C. Hui, L. H. Bao, C. Li, Y. Tian, H. Ding, C. M. Shen and H. J. Gao, *Appl. Phys. Lett.*, 2009, **94**, 083101-1-3.
12 F. Liu, P. J. Cao, H. R. Zhang, J. Q. Li and H. J. Gao, *Nanotechnology*, 2004, **15**, 949–952.
13 H. B. Zeng, W. P. Cai, Y. Li, J. L. Hu and P. S. Liu, *J. Phys. Chem. B*, 2005, **109**, 18260–18266.
14 W. A. H. Bentley, W. J., *Snow Crystal*, Harvard University Press, Cambridge, 1954.
15 M. N. Popescu, H. G. E. Hentschel and F. Family, *Phys. Rev. E*, 2004, **69**, 061403-1-6.
16 M. Hohage, M. Bott, M. Morgenstern, Z. Y. Zhang, T. Michely and G. Comsa, *Phys. Rev. Lett.*, 1996, **76**, 2366–2369.
17 H. Brune, H. Roder, K. Bromann, K. Kern, J. Jacobsen, P. Stoltze, K. Jacobsen and J. Norskov, *Surf. Sci.*, 1996, **349**, L115–L122.
18 H. Brune, C. Romainczyk, H. Roder and K. Kern, *Nature*, 1994, **369**, 469–471.
19 J. Nittmann and H. E. Stanley, *J. Phys. A: Math. Gen.*, 1987, **20**, L1185–L1191.
20 J. Kertesz and T. Vicsek, *J. Phys. A: Math. Gen.*, 1986, **19**, L257–L262.
21 L. M. Sander, *Contemp. Phys.*, 2000, **41**, 203–218.
22 J. X. Zhong, T. J. Zhang, Z. Y. Zhang and M. G. Lagally, *Phys. Rev. B*, 2001, **63**, 113403-1-4.
23 Z. Y. Zhang and M. G. Lagally, *Science*, 1997, **276**, 377–383.

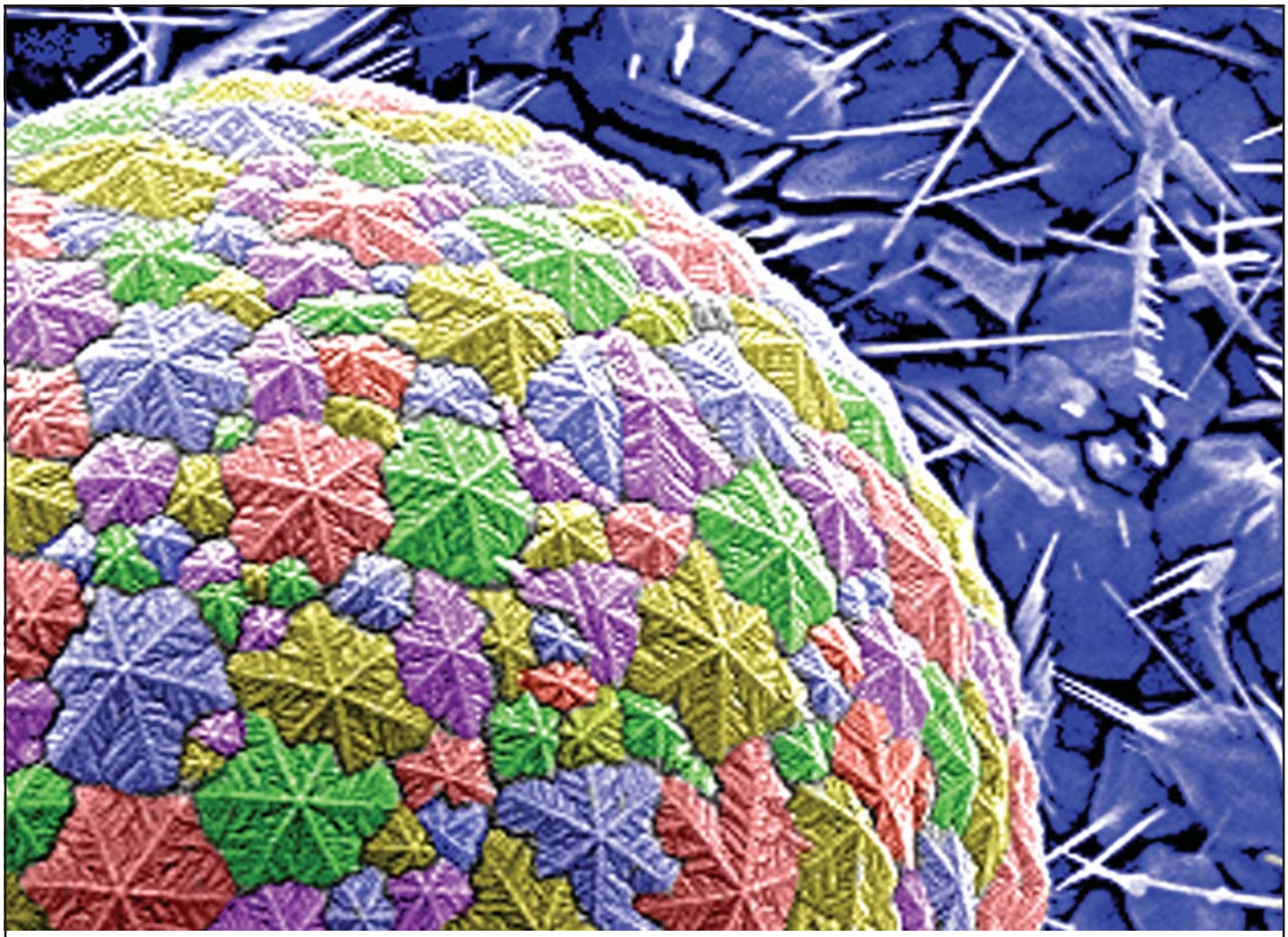

Showcasing research from the Institute of Physics, Chinese Academy of Sciences, Beijing, China.

Title: Atomic-scale tuning of self-assembled ZnO microscopic patterns: from dendritic fractals to compact islands

Highly regular and symmetric dendritic snowflake patterns and smooth compact islands were obtained at different growth conditions in the growth of ZnO *via* chemical vapor deposition. These dendritic patterns were reproduced using atomistic Monte Carlo simulations. We employed the ZnO to mimic successfully nature's versatility in creating microscopic patterns with tunable morphology.

As featured in:

See Gao *et al.*, *Nanoscale*, 2010, **2**, 2557.

RSCPublishing

www.rsc.org/nanoscale

Registered Charity Number 207890